JCB Article

A novel p21-activated kinase binds the actin and microtubule networks and induces microtubule stabilization

Julien Cau,[1] Sandrine Faure,[1] Michel Comps,[2] Claude Delsert,[2] and Nathalie Morin[1]

[1]Centre de Recherche de Biochimie Macromoleculaire, Centre National de la Recherche Scientifique UPR 1086, 34293 Montpellier cedex 5, France
[2]French Research Institute for Exploitation of the Sea (IFREMER), 17390 La Tremblade, France

Coordination of the different cytoskeleton networks in the cell is of central importance for morphogenesis, organelle transport, and motility. The Rho family proteins are well characterized for their effects on the actin cytoskeleton, but increasing evidence indicates that they may also control microtubule (MT) dynamics. Here, we demonstrate that a novel Cdc42/Rac effector, X-p21-activated kinase (PAK)5, colocalizes and binds to both the actin and MT networks and that its subcellular localization is regulated during cell cycle progression. In transfected cells, X-PAK5 promotes the formation of stabilized MTs that are associated in bundles and interferes with MTs dynamics, slowing both the elongation and shrinkage rates and inducing long paused periods. X-PAK5 subcellular localization is regulated tightly, since coexpression with active Rac or Cdc42 induces its shuttling to actin-rich structures. Thus, X-PAK5 is a novel MT-associated protein that may communicate between the actin and MT networks during cellular responses to environmental conditions.

Introduction

The major components of the cytoskeleton belong to three networks: the actin filaments (MFs), microtubules (MTs),* and intermediate filaments (IFs). These are dynamic structures that cooperate in the cell response to extracellular stimuli and allow the cell to modulate its shape, to migrate, and to divide. The Rho GTPases are tightly involved in the coordination of these networks. Indeed, Rho, Rac, and Cdc42 are best known for the control they exert on cell shape and mobility by regulating the actin cytoskeleton. Cdc42 and Rac1 trigger the formation of filipodia and lamellipodia, respectively, whereas RhoA stimulates the assembly of contractile actin stress fibers. All three GTPases regulate the assembly of focal contacts and thus the adhesion properties of the cell to the extracellular matrix (Nobes and Hall, 1995).

Nonetheless, GTPases are also linked to MT dynamics. Indeed, growing MTs target Rho-dependent focal adhesions and regulate their turnover (Kaverina et al., 1998, 1999). MT depolymerization induces RhoA activation and the subsequent formation of stress fibers (Enomoto, 1996), and active RhoA stabilizes a subset of MTs during cell polarization (Cook et al., 1998; Palazzo et al., 2001). It is also known that Rac binds tubulin (Best et al., 1996) and the activation of Rac is associated with the recovery of fibroblasts from nocodazole (NZ) treatment (Waterman-Storer et al., 1999). Finally, reorientation of the MT organizing center that occurs during wounding depends on the activation of a Cdc42/dynein/dynactin pathway (Etienne-Manneville and Hall, 2001).

p21-activated kinases (PAKs) are well-characterized effectors of Rac and Cdc42 (Manser et al., 1994). Upon binding to active GTPase, PAK1–3 undergo a conformational change that allows their autophosphorylation and activation, whereas hPAK4 relocates within the cell upon GTPase binding (Abo et al., 1998). PAKs are involved in the regulation of cell cycle (Faure et al., 1997, 1999; Cau et al., 2000), apoptosis (Faure et al., 1997; Manser and Lim, 1999), and in mediating actin cytoskeleton reorganization (for review see Bagrodia and Cerione, 1999; Daniels and Bokoch, 1999; Manser and Lim, 1999). PAKs also regulate cell motility. This likely occurs by

The online version of this article contains supplemental material.

Address correspondence to Nathalie Morin, Centre de Recherche de Biochimie Macromoleculaire, CNRS UPR 1086, 1919 Route de Mende, 34293 Montpellier cedex 5, France. Tel.: 33-4-6761-3330. Fax: 33-4-6752-1559. E-mail: morin@crbm.cnrs-mop.fr

*Abbreviations used in this paper: IF, intermediate filament; MAP, MT-associated protein; MF, actin filament; MT, microtubule; NZ, nocodazole; PAK, p21-activated kinase.

Key words: PAK; actin; microtubules; stabilization; dynamics

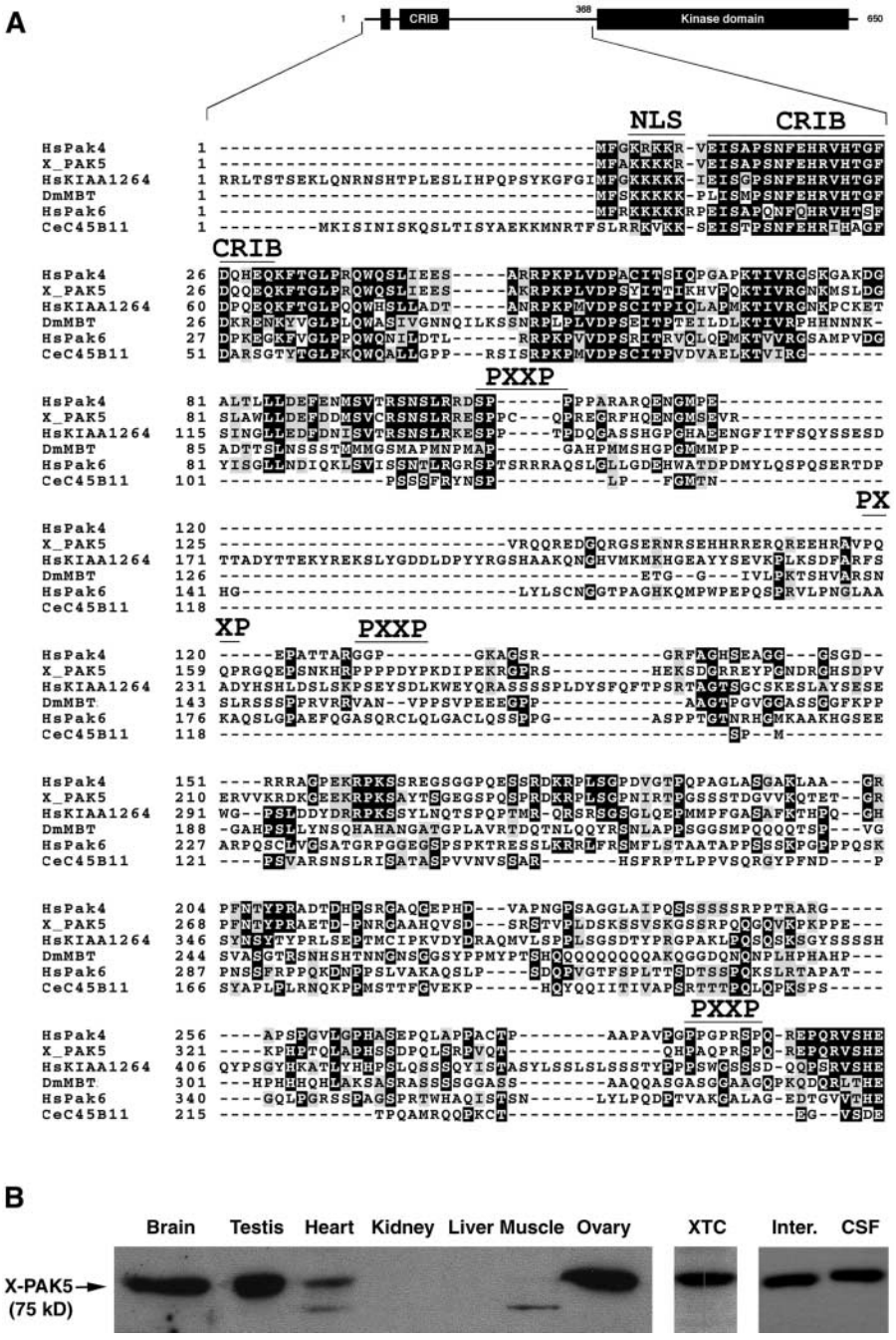

Figure 1. **X-PAK5 belongs to a new PAK subfamily.** (A) Multiple sequences alignment (ClustalW) of X-PAK5 NH2-terminal amino acid sequence with that of hsPAK4 (AJ011855), KIAA1264 (BAA86578), hsPAK6 (NP_064553), DmMBT (AJ011578), and CeC45B11 (Z74029); amino acids identity and homology are black and gray boxed, respectively. A putative nuclear localization sequence (NLS), CRIB domain, and potential SH3 binding domains (PXXP) are indicated. (B) Western blot was performed on interphase (inter) or CSF Xenopus egg, XTC cells, and Xenopus tissues extracts using immunopurified Abn122.

controlling the actin dynamics and contraction, since LIM kinase and myosin II light chain were identified as PAK substrates (Edwards et al., 1999; Zeng et al., 2000).

Recent reports suggest that PAKs may also regulate the IF and MT networks. Indeed, desmin was identified as a PAK substrate (Ohtakara et al., 2000), and a yet unidentified PAK mediates Rac/Cdc42-induced inactivation of stathmin (Daub et al., 2001). Finally, expression of an active PAK in breast epithelial cells induced abnormal mitotic spindles in 10% of the cells (Vadlamundi et al., 2000). This led us to investigate the relationships of a novel *Xenopus* PAK, X-PAK5, with the cell cytoskeleton networks.

Here, we demonstrate that endogenous X-PAK5 binds the actin and MT networks. X-PAK5 subcellular localization is regulated during cell cycle, and a subset of the protein associates with spindle MTs. Ectopically expressed X-PAK5 associates either with curly MTs or stress fibers and lamellipodia. Catalytically inactive X-PAK5 reorganizes the MT

Figure 2. **Endogenous X-PAK5 subcellular localization and regulation during cell cycle progression.** X-PAK5 subcellular localization was analyzed using immunopurified Abn122 in XTC cells. (A) Subset of X-PAK5 colocalizes with the Golgi apparatus. (B) X-PAK5 costains with actin and tubulin networks. Square regions 1 and 2 were selected on the merged image between X-PAK5 (green), MTs (red), and actin (blue) networks to perform quantitative colocalization. (a) X-PAK5 (green) colocalization in square 1 with microfilaments (blue); white spots represent colocalized voxels. (b) X-PAK5 (green) colocalization in square 1 with MTs (red). Yellow spots represent colocalized voxels. (C) X-PAK5 costains with vimentin and tubulin networks. Square region 3 was selected on the merged image between X-PAK5 (green), MTs (red), and

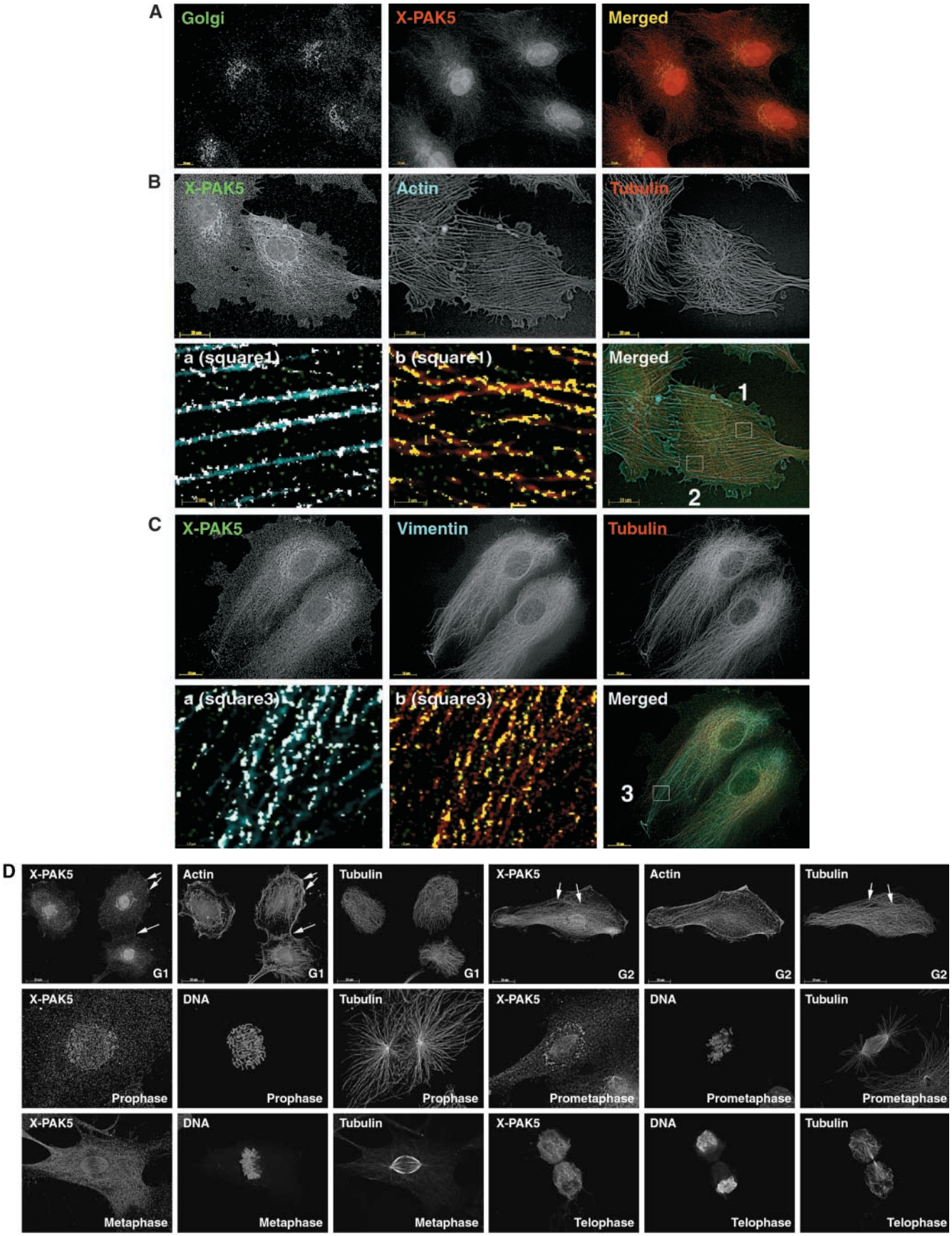

vimentin (blue) networks. (a) X-PAK5 (green) colocalization with vimentin (blue); white spots represent colocalized voxels. (b) X-PAK5 (green) colocalization with MTs (red). Yellow spots represent colocalized voxels. (D) Representative G1 and G2 cells illustrate the more or less filamentous pattern of X-PAK5 during cell cycle progression. Cells were triple stained for X-PAK5, actin, and tubulin in G1 and G2. Arrows show actin-rich structures or single MTs decorated by X-PAK5. During mitosis, cells were triple stained for X-PAK5, DNA, and tubulin.

network and induces its stabilization. X-PAK5 binding to the MTs is lost when catalytic activation occurs. Finally, Cdc42/Rac GTPases do not regulate X-PAK5 catalytic activation but induce its shuttling from the MTs toward actin-rich structures. Therefore, X-PAK5 may represent a functional link in the coordinated dynamics of these networks.

Results

X-PAK5 cloning and expression pattern

In an attempt to identify new members of the PAK family in *Xenopus*, we cloned a 2049 bp cDNA, containing an ORF that encodes a predicted 649 amino acid protein. This putative protein and hPAK4 share almost identical CRIB domains, show 92.6% identity in their kinase domain, and form a new PAK subfamily that also includes four other related sequences (Fig. 1 A). However, its sequence differs from hPAK4 by a 103 amino acid insert at position 122 that contains 50% acidic and basic amino acids. Therefore, we named this new protein X-PAK5.

A polyclonal antibody (Abn122) raised against the unique 122–224 domain reacts specifically with a single band of 75 kD in *Xenopus* egg extracts and XTC cells, consistent with the 73.6 kD predicted molecular weight of the ORF. This protein is expressed mainly in brain, ovary, and testis, although a smaller immunologically related protein is detected in muscle and heart (Fig. 1 B).

Subpopulations of X-PAK5 bind the actin and MT cytoskeleton networks

X-PAK5 subcellular localization was examined in XTC cells. X-PAK5 is localized both in the nucleus and cytoplasmic compartments (Fig. 2 A). In the cytoplasm, X-PAK5 colocalized with the Golgi apparatus (Fig. 2 A) and was either punctate stained or distributed along more organized filamentous structures (Fig. 2, A and B).

To identify the cytoplasmic structures to which X-PAK5 is segregated, we compared the distribution of X-PAK5 with that of the three major cytoplasmic filamentous networks: the MTs, MFs, and IFs (Fig. 2, B and C). Codistribution between MFs, MTs, and X-PAK5 was calculated on every plane of the selected region 1 (Fig. 2 B, merged). Quantification (unpublished data; see Materials and methods) demonstrates that in this area of the cell X-PAK5 colocalization with MTs (Fig. 2 B, b) and with MFs (Fig. 2 B, a) was highly significant (Fig. 2 B, a, white, and B, b, yellow), whereas some triple colocalization is also observed between MFs, MTs, and X-PAK5. The same analysis performed between IFs, MTs, and X-PAK5 (Fig. 2 C) revealed that in the chosen region 3 X-PAK5 colocalizes with the IF networks (Fig. 2 C, a and b). Nevertheless, as most of the IFs in this region of the cell are coaligned with MTs it is difficult at this point to conclude whether X-PAK5 colocalizes with the MTs or IFs or both. It is noteworthy that X-PAK5 is not uniquely colocalized with either filament network. For example, no significant colocalization could be detected in the selected region 2 (Fig. 2 B; unpublished data). Thus, these highly sensitive analyses demonstrate that X-PAK5 can colocalize specifically with subsets of either MTs and IF or with actin MFs.

Table I. **X-PAK5 filamentous staining during cell cycle progression**

	Filamentous staining	n[a]
	%	
G0	11.48	211
G1	15.62	207
S	63.96	242
G2	72.46	185

[a]n, total number of cell counted.

Because the staining of X-PAK5 is punctate or filamentous in XTC cells, we wondered if its distribution could be regulated during cell cycle progression (Fig. 2 D). In quiescent-starved and G1-synchronized XL2 cells, X-PAK5 was distributed mainly in the nucleus, Golgi, and lamellipodia and was scattered and punctate in the cytoplasm. During S (unpublished data) and G2, X-PAK5 binding along the MTs/IFs increased dramatically. This filamentous staining of X-PAK5 along the MT/IFs tracks was easily recognizable under the microscope. Quantitation (Table I) demonstrates that X-PAK5 was increasingly associated with the MT/IF networks as the cell cycle progressed. Finally, when the cells entered mitosis (Fig. 2 D) X-PAK5 did not associate with the aster MTs during prophase but labeled the spindle MTs from prometaphase to anaphase. X-PAK5 associated with the nucleus and Golgi compartments from G1 to G2, although filamentous staining somehow disturbed our ability to detect this in G2.

Thus, together our results demonstrate that endogenous X-PAK5 is the first PAK family member that colocalizes with both the MF and MT/IF filament networks within the cell and whose distribution is regulated during cell cycle progression.

X-PAK5 binds to MT and filamentous actin through its regulatory domain

To further confirm our results, we undertook different biochemical approaches. First, to assess whether endogenous X-PAK5 is bound to the MT in *Xenopus* egg extracts we purified the MTs and associated protein fraction (P) from a high speed supernatant of *Xenopus* egg extract depleted of F-actin and IFs and treated with taxol. The P fraction was compared with the total (T) and MT/MT-associated protein (MAP)–depleted supernatants (S) for the presence of β-tubulin, Cdk2 (a control protein that does not bind to MTs), and X-PAK5. Unlike Cdk2, a fraction of X-PAK5 associated and cosedimented with the taxol-stabilized MTs. When MT polymerization was inhibited in NZ-treated extracts, neither tubulin nor X-PAK5 sedimented through the glycerol cushion, indicating that X-PAK5 pull-down requires MTs (Fig. 3 A). Up to 70% of endogenous X-PAK5 bound to the MTs (Fig. 3 A). Thus, these experiments establish that X-PAK5 is indeed bound to MTs in egg extracts.

Next, to ascertain which region of X-PAK5 binds MTs in vitro–translated and tagged regulatory (Nter) or kinase (Cter) domains were added to the egg extracts. Our data show that the regulatory domain is responsible for the binding to the MTs (Fig. 3 B). Furthermore, binding occurred with the in vitro–translated wild-type (wt) and kinase dead (K/R; see Fig. 9 A for activities) mutant, showing that cata-

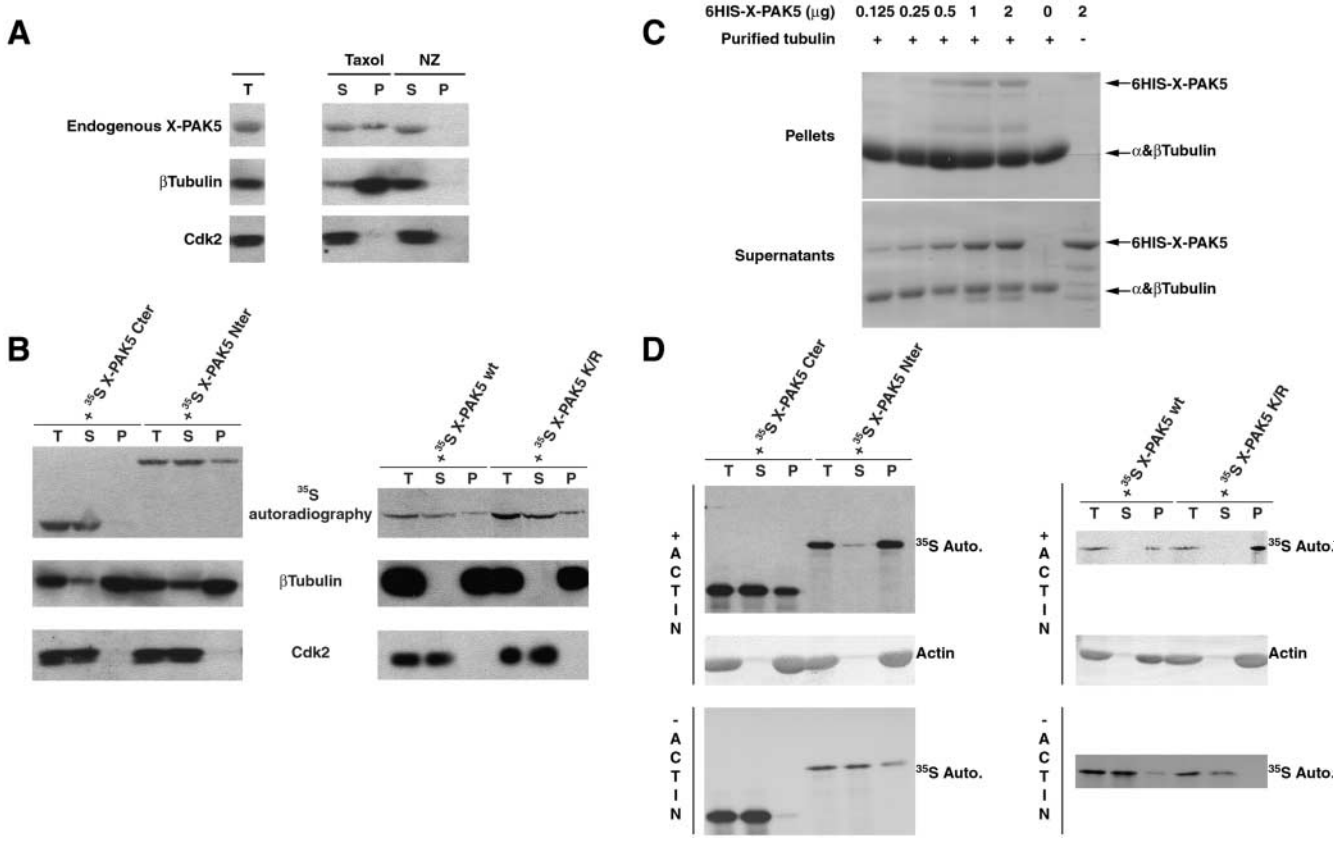

Figure 3. **X-PAK5 binds MTs and MFs.** (A and B) Western blot analysis of MTs copelleting assays. 2 ml equivalent of the pellet fraction (P), the depleted supernatant (S), and the high speed egg extract (T) are loaded in all lanes. Nitrocellulose was probed with b tubulin (E7), Abn122, and cdk2 antibodies. Autoradiography allowed detection of in vitro–translated X-PAK5 mutants. (A) Endogenous X-PAK5 associates to taxol stabilized MTs (Taxol) but is not pelleted in NZ-treated extracts (NZ). (B) 35S X-PAK5 wt and 35S X-PAK5 K/R associate to MTs. Binding occurs through the N-Ter regulatory domain (^{35}S X-PAK5 Nter) but not through the C-ter catalytic domain (^{35}S X-PAK5 Cter). (C) Recombinant His6-tagged X-PAK5 (0.1–2 μg) was incubated with MTs (20 μg) polymerized from purified brain tubulin, and MTs were pelleted. Supernatants and pellets were loaded on SDS-PAGE that was Coomassie stained. (D) Actin spin-down binding assays with the in vitro–translated X-PAK5 mutants. Most of wt (^{35}S X-PAK5 wt) and kinase dead X-PAK5 (^{35}S X-PAK5 K/R) bind to polymerized MFs. Binding occurs through the N-ter domain, but the C-ter domain also binds microfilaments to some extent. In absence of actin (−actin, bottom) most of the in vitro–translated product was recovered in the supernatant fraction. Experiments in Fig. 3 are representative of at least three experiments.

lytic activity of the kinase is not required for its binding to the MTs (Fig. 3 B).

Finally, we asked whether X-PAK5–MT binding was direct. MTs were assembled from purified brain tubulin, incubated with purified His_6-tagged X-PAK5, and purified as above. Increasing quantities of His_6–X-PAK5 corresponded to greater association with polymerized tubulin in the pellet fraction, indicating that X-PAK5 binding is actually dose dependent (Fig. 3 C).

Taken together, these results confirmed and extended our previous conclusions that X-PAK5 is a novel MAP that binds directly to MTs.

We further analyzed the binding of X-PAK5 to F-actin using an in vitro assay. Full-length X-PAK5 cosedimented with filamentous actin independently of its catalytic activity (Fig. 3 D). Both the regulatory and kinase domains of X-PAK5 bound F-actin, although the relative binding efficiency of the COOH-terminal domain was quite low in comparison to the regulatory domain. Control reactions showed that essentially none of the in vitro–translated products pelleted in the absence of F-actin (Fig. 3 D). This in vitro assay confirmed that X-PAK5 binds, at least indirectly, to F-actin.

Overexpressed X-PAK5 binds both the actin and the MT cytoskeleton networks

To gain further insight into the role and biological activities of X-PAK5, we expressed wt GFP-tagged X-PAK5 into XTC cells (Fig. 4). 24 h after transfection, the overexpression of the wt kinase was estimated to be five- to sixfold (unpublished data). In 51.8% of the cells overexpressing the fusion protein, MTs appeared to be fewer relative to untransfected neighboring cells but also thicker as if associated in bundles. GFP–X-PAK5 decorated a large number of these curly MTs (Fig. 4 A) and was also associated with small round particles, unlikely to be amorphous, since some of them moved along MT tracks (unpublished data). In these cells, stress fibers were often less numerous, whereas actin reorganized cortically and IFs aggregated around the nucleus (Fig. 4 B). GFP–X-PAK5–bound MTs did not colocalize with the collapsed IFs, further demonstrating its specific binding to MTs rather than IFs.

In 9.8% of the transfected cells, the MT network appeared unaffected and GFP–X-PAK5 localized to lamellipodia and bound to thin stress fibers (Fig. 4 C). In the remaining transfected cells, again X-PAK5 was associated with

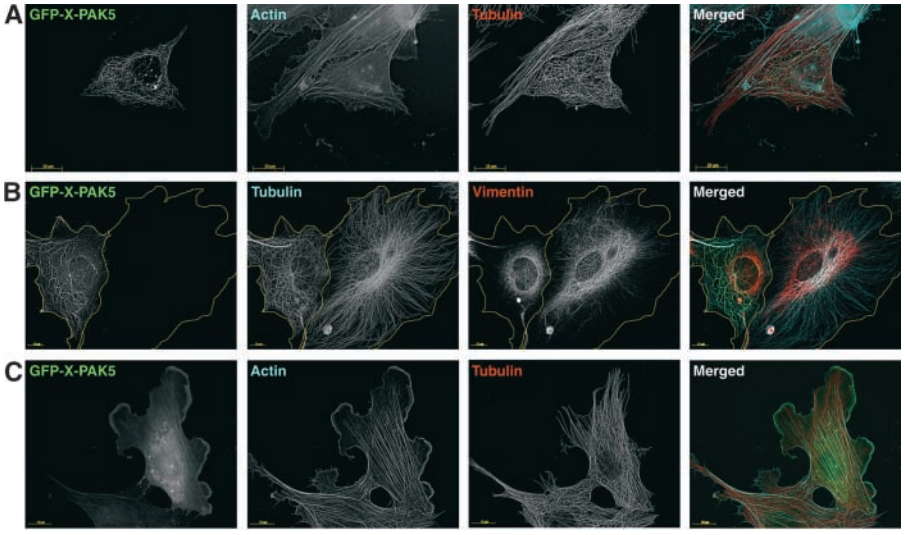

Figure 4. **X-PAK5 disorganizes the actin and MTs networks.** XTC cells transfected with GFP–X-PAK5 were costained for actin (blue), IFs (red), and tubulin (red). (A) In 51.8% of transfected cells ($n = 162$), X-PAK5 colocalizes with the disorganized MTs. (B) When X-PAK5 colocalizes with MTs, IFs are collapsed (in 85% of transfected cells, $n = 120$), whereas only 32% ($n = 260$) of untransfected cells had a similar phenotype. (C) In 9.8% of transfected cells ($n = 162$), X-PAK5 colocalizes with actin stress fibers and lamellipodia.

small particles in the cytoplasm (unpublished data). Thus, the experiments presented here show that ectopic GFP–X-PAK5, like the endogenous kinase, primarily associates with the MTs and to a smaller extent with the actin network.

We then focused our study on the mechanisms by which GFP–X-PAK5 induces the striking changes observed in the morphology and the organization of MTs.

GFP–X-PAK5 induces a decrease of the Tyr/Glu MTs ratio

In polarized and differentiated cells, a fraction of MTs become stabilized and undergo many posttranslational modifications such as detyrosination by a carboxypeptidase that leads to GluMTs. To determine whether X-PAK5 might induce MTs stabilization, we compared the dynamic tyrosinated (TyrMT) and stabilized detyrosinated (GluMTs) subpopulations in GFP–X-PAK5–expressing cells versus untransfected cells.

As shown in Fig. 5 A, X-PAK5 partially colocalized with both TyrMT and GluMT subspecies. GluMTs were often restricted to the perinuclear region of the cell and like in nonmotile cells did not extend to its edges (Nagasaki et al., 1992); whereas TyrMTs were mostly excluded from this region. TyrMTs were often stained to a lower extent and undetectable in some of X-PAK5–expressing cells (unpublished data).

To quantify Tyr and Glu staining, we compared the ratios of TyrMTs/GluMTs (Ratio R1) subpopulations in a transfected cell to the average ratio obtained from all untransfected cells in the same field (average ratio R2) (Fig. 5 B). In comparison with control GFP-expressing cells, the average R1/R2 value calculated in GFP–X-PAK5–expressing cells was ~25% lower. Thus, such a significant difference suggests that GFP–X-PAK5 binding to the MTs may affect either their stability or posttranslational modifications.

Stability of GFP–X-PAK5–bound MTs to dilution-induced depolymerization

GluMTs are stabilized MTs, although the carboxypeptidase activity generating the GluMTs is not responsible for their stabilization (Cook et al., 1998). Indeed, Infante et al. (2000) showed that MT capping is responsible for MT stabilization.

To test whether X-PAK5–bound MTs were stabilized, GFP–X-PAK5–transfected cells were detergent extracted and immediately fixed or incubated for 30 min before fixation (Fig. 6). Under these conditions, dynamic MTs with high turnover disappear rapidly, since the free tubulin released is too diluted to be reincorporated. In contrast, stable MTs with slow turnover are less affected and can be stained after fixation. TyrMTs stained immediately after cell extraction were not affected significantly and colocalized partially with X-PAK5. In contrast, after 30 min a complete turnover of dynamic MTs had occurred, since no TyrAb staining could be detected in any of the untransfected cells. In contrast, GFP–X-PAK5–bound MTs resisted the dilution treatment, remained labeled, and partially costained with TyrAbs, which indicates that X-PAK5 binding allows MTs that are not yet completely detyrosinated to be stabilized.

X-PAK5 binds to nucleating MTs and induces their dynamic and morphological changes

To further confirm a function of X-PAK5 in MT stabilization, GFP–X-PAK5–transfected cells were treated for 1 h with NZ. Then, new growth of MTs was induced by NZ wash out (Fig. 7 A). After a 15-min recovery, X-PAK5 associated with newly growing TyrMTs. To assess whether these newly formed MTs could be stabilized by X-PAK5 binding, we performed time-lapse microscopy on live GFP–X-PAK5–transfected A6 cells and used A6 cells stably expressing GFP–β-tubulin (H1H10 cells) (Mimori-Kiyosue et al., 2000) as controls. In H1H10 cells, virtually all MTs depolymerized within 20 min of NZ treatment, and a complete MT network was regrown by 10 min recovery (unpublished data). In contrast, X-PAK5–bound MTs were strongly resistant to NZ as seen on frames recorded at 0 and 30 min and 1 and 2 h after NZ treatment (Fig. 7 B; videos 1 and 2 available at http://www.jcb.org/cgi/content/full/jcb.200104123/DC1). We verified, using RFP–X-PAK5–transfected H1H10, that NZ-resistant X-PAK5–labeled filaments were indeed MTs (unpublished data). Wash out was performed after 2.5–3 h of drug treatment. Frames recorded after 0, 8,

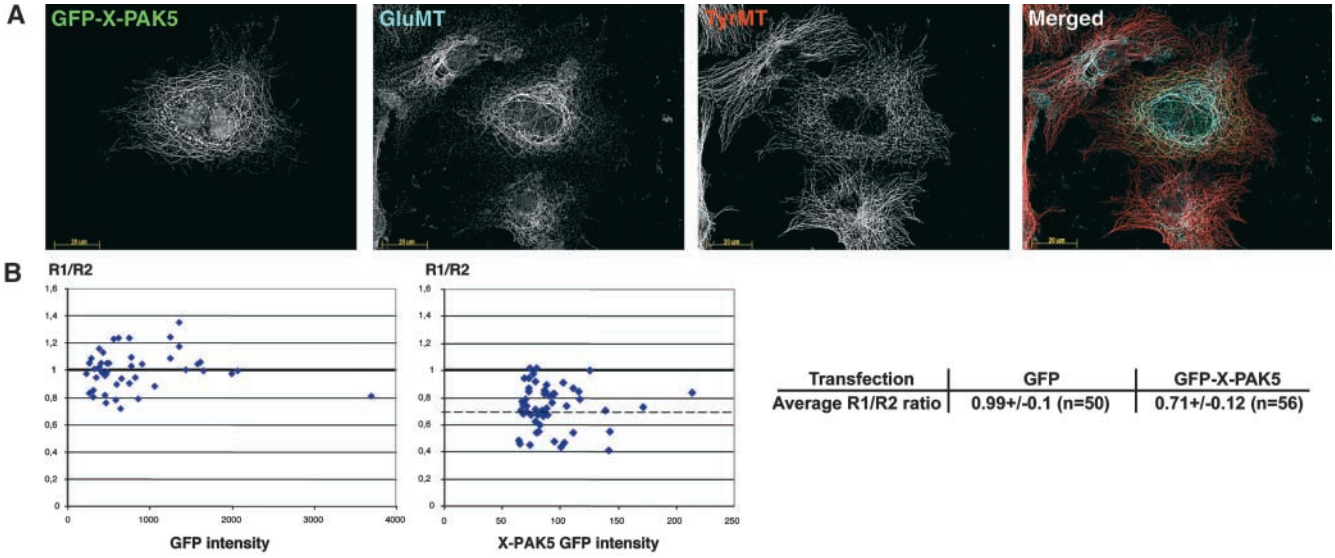

Figure 5. **X-PAK5 rearranges the MT network.** XTC cells were transfected with GFP–X-PAK5 and stained with specific antibodies against TyrMTs and GluMTs (A). (B) The R1/R2 ratios in GFP- (left) or GFP–X-PAK5– (middle) transfected cells are plotted against GFP intensity. R1/R2 was below 1 for most GFP–X-PAK5–transfected cells.

and 15 min and 1 h 40 min recovery show that X-PAK5 bound newly formed MTs nucleating from the centrosome after the drug wash out (Fig. 7 B; videos 1 and 2 available at http://www.jcb.org/cgi/content/full/jcb.200104123/DC1). However, X-PAK5–bound MTs elongated very slowly over time, as best seen in the centrosome enlarged region, consistent with the hypothesis that X-PAK5 binding to MTs induced their stabilization.

GFP–X-PAK5 affects MT dynamics

To determine whether X-PAK5 acts as a conventional MAP by interfering with MTs dynamic properties, we measured MT dynamic and pausing properties either in control H1H10 cells or on GFP–X-PAK5–bound MTs from A6 cells (Fig. 8; videos 3–5 available at http://www.jcb.org/cgi/content/full/jcb.200104123/DC1; Table II). In contrast to control GFP-bound MTs (Fig. 8 A; video 3 available at http://www.jcb.org/cgi/content/full/jcb.200104123/DC1), GFP–X-PAK5–bound MTs in A6 cells were paused most of the time and showed very reduced growth and shrinkage rates (Fig. 8 B). However, neither the catastrophe nor the rescue frequency were affected significantly (Fig. 8 B; video 4 available at http://www.jcb.org/cgi/content/full/jcb.200104123/DC1; Table II). Nevertheless, because MTs were not labeled directly it was unclear whether GFP–X-PAK5 was bound along the entire length of MTs up to their plus end. Thus, these measures were potentially not representative of the dynamics of X-PAK5 bound MTs. To address this question, we used H1H10 cells transiently expressing RFP–X-PAK5 (Fig. 8 C). GFP-labeled MTs that did not bind RFP–X-PAK5 displayed the same dynamic as in untransfected cells, whereas elongation and shortening rates of the RFP–X-PAK5–bound GFP-labeled MTs (that appear yellow and much thicker) were affected (Fig. 8 C; video 5 available at http://www.jcb.org/cgi/content/full/jcb.200104123/DC1; Table II). Those dynamic values were comparable to the ones obtained with GFP–X-PAK5–bound MTs in A6 cells. However the speed of elongation and shrinkage were so reduced that these measured rates are very close to the detection limits of our assay. Strikingly, during 80% of the recording time X-PAK5–bound MTs were neither growing nor shrinking but paused. The time

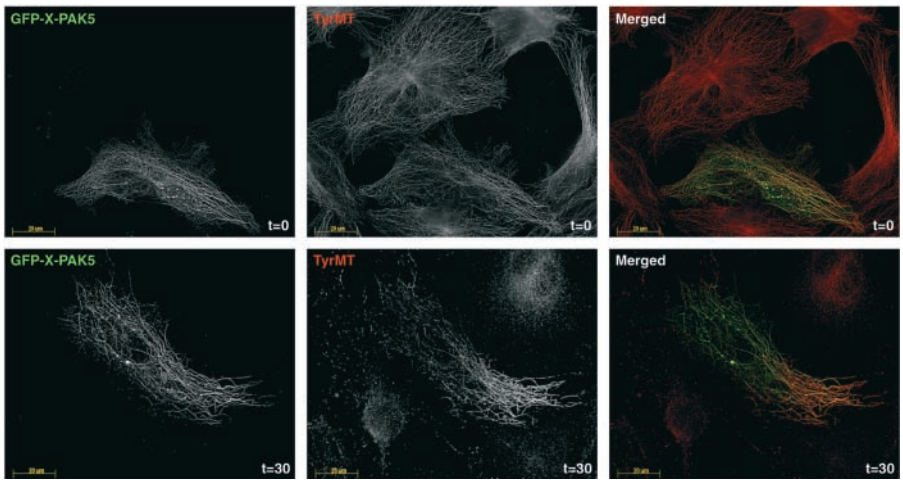

Figure 6. **X-PAK5–bound MTs are stable against dilution-induced depolymerization.** GFP–X-PAK5–transfected XTC cells were permeabilized and immediately fixed ($t = 0$, top) or incubated in PEM buffer for 30 min ($t = 30$, bottom) and fixed. GFP–X-PAK5 was costained with TyrMTs.

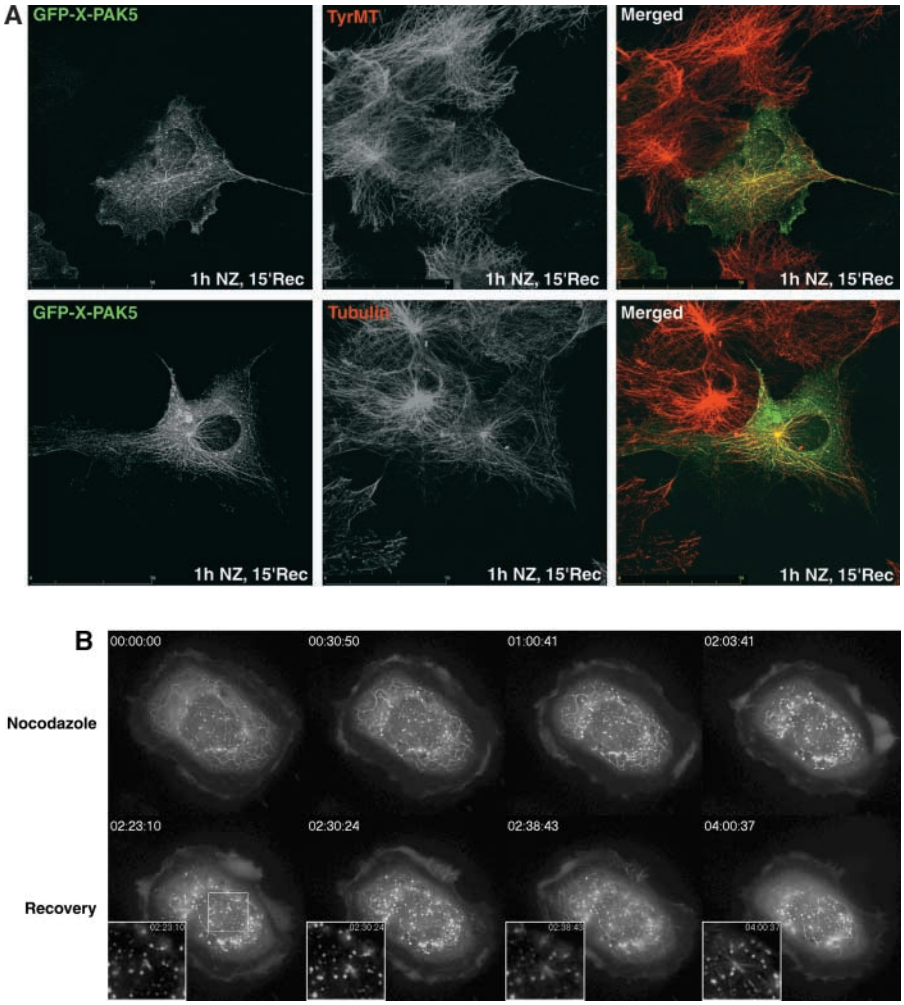

Figure 7. **X-PAK5 associates to newly nucleating MTs and induces their morphological change.** (A) GFP–X-PAK5–transfected XTC cells were treated with 10 μM NZ for 1 h, washed in fresh medium for 15 min (1 h NZ, 15′Rec), and stained for TyrMTs (top) or MTs (bottom). Merged images are on the right. (B) GFP–X-PAK5–transfected XTC cells were treated with 10 μM NZ for 2.2 h and washed for 2 h more. Live cell behavior was recorded by time-lapse microscopy (see videos 1 and 2 http://www.jcb.org/cgi/content/full/jcb.200104123/DC1 for the zoomed region). GFP–X-PAK5–bound MTs are seen at 0 and 30 min and 1 and 2 h after NZ treatment and after 0, 8, and 15 min and 2 h recovery. The area surrounding the centrosome is magnified in recovery time points.

MTs spent paused represented an eightfold increase compared with GFP MTs. (These data obtained by following an average of 50 MTs are summarized in Table II.) In summary, our results indicate that X-PAK5 is a novel MT binding protein that promotes MT pause and stabilized MTs.

Catalytic activation of X-PAK5 prevents its MT stabilizing activity

To determine whether X-PAK5 kinase activity was required to induce MT stabilization, we generated GFP–X-PAK5/EN, a mutant carrying two point mutations in the putative autophosphorylation site and catalytic loop of the kinase. These mutations were shown previously to constitutively activate hPAK4 (Qu et al., 2001). The kinase activity of this mutant was tested together with that of the wt and kinase dead GFP–X-PAK5. H2B phosphorylation in GFP–X-PAK5K/R- and mock-transfected cells are comparable and likely represent the level of activity of the endogenous X-PAK5 kinase that is measured together with the ectopic kinase (Fig. 9 A). Since the increase of H2B

Table II. **Dynamic properties of X-PAK5–bound MTs**

	H1H10	A6	H1H10	
	GFP-MTs[a]	GFP–X-PAK5 MTs[b]	GFP-MTs[c]	RFP–X-PAK5 MTs[d]
Growth rate (μm/min^{-1})	8.88 ± 2.10	3.66 ± 0.95	10.27 ± 1.88	3.61 ± 0.54
Shrinkage rate (μm/min^{-1})	9.98 ± 2.12	3.42 ± 0.72	11.69 ± 2.44	3.25 ± 0.75
Rescue frequency (Res/min^{-1})	3.67 ± 1.02	1.60 ± 0.85	3.83 ± 0.73	1.55 ± 0.80
Catastrophe frequency (Cat/min^{-1})	3.37 ± 0.94	2.21 ± 0.73	4.09 ± 0.73	1.99 ± 0.50
Growth (%)	49.73 ± 6.11	10.53 ± 6.07	46.77 ± 11.00	9.05 ± 4.16
Shrinkage (%)	40.99 ± 10.37	13.30 ± 6.07	48.97 ± 11.01	10.60 ± 3.27
Pausing (%)	9.2 ± 0.40	76.18 ± 11.48	4.26 ± 2.89	80.24 ± 5.74

[a] $n = 55$ (20 cells).
[b] $n = 42$ (17 cells).
[c] $n = 50$ (20 cells).
[d] $n = 51$ (20 cells).

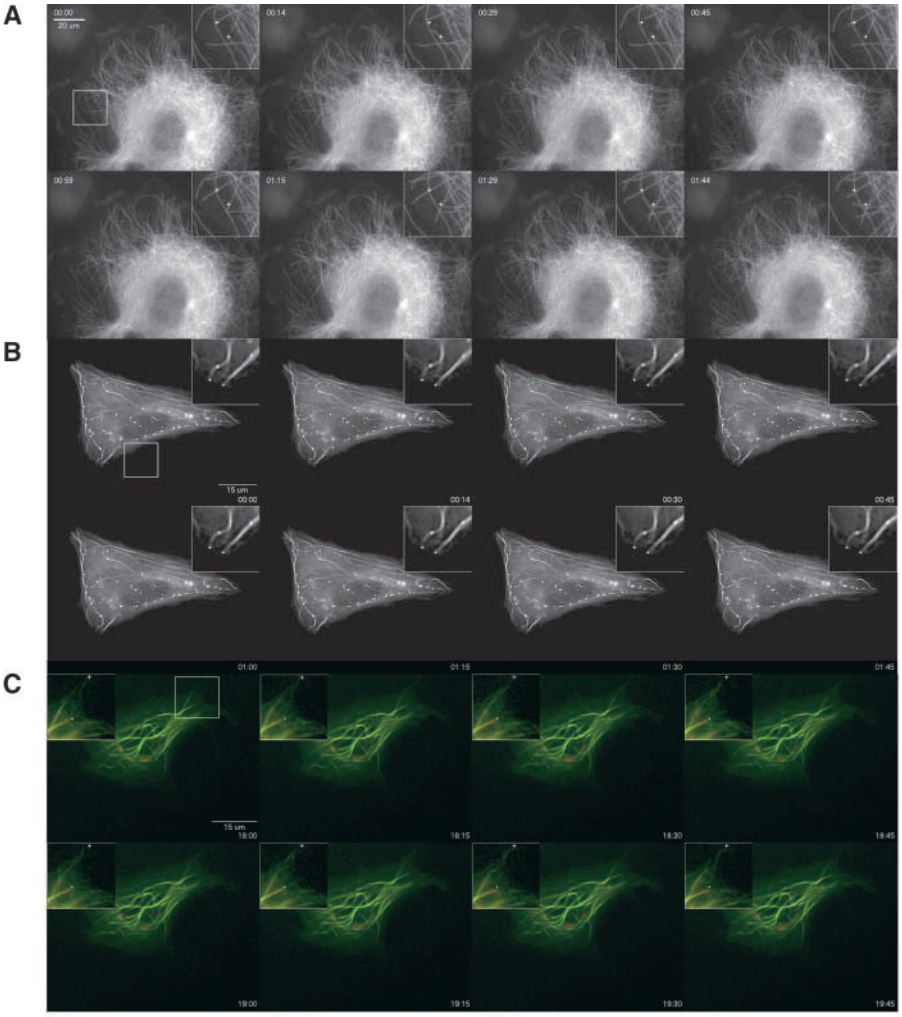

Figure 8. **Dynamic of MTs in A6 and H1H10 cells.** Elapsed time is indicated at the top left (A) and bottom right (B and C) (min:sec). (A) Dynamic of GFP-labeled MTs in live H1H10 cells. The boxed area is zoomed on the top right; the cross pinpoints the initial position of one MT. Also see video 3. (B) Dynamics of GFP–X-PAK5–bound MTs in live A6 cells. The boxed area is zoomed on the top right. The two crosses pinpoint at two thick GFP–X-PAK5–bound MTs that essentially stay still and paused. Also see video 4. (C) Dynamic of RFP–X-PAK5–bound GFP MT bundles (the dot pinpoints the initial position of the free end of a bundle) versus unbound GFP MTs (the cross pinpoints the initial position of one MT) were overlaid. Also see video 5; all videos available at http://www.jcb.org/cgi/content/full/jcb.200104123/DC1.

phosphorylation is less than twofold compared with the dead kinase in wt GFP–X-PAK5–transfected cells, the latter is either poorly activated or inactivated under these conditions of expression. In contrast, GFP–X-PAK5/EN mutant is constitutively active as seen by a 30-fold increase of H2B phosphorylation. Immunoblotting of the immunoprecipitates revealed that the three proteins were expressed at comparable levels (Fig. 9 A).

The two mutants were expressed in XTC cells to study the catalytic activity requirements for MTs binding and stabilizing activities. GFP–X-PAK5K/R bound to MTs with the same efficiency as the wt kinase (Fig. 9 B), which confirms our biochemical evidence (Fig. 3). Morphological changes (Fig. 9 B) and dynamic behavior of GFP–X-PAK5/KR–bound MTs (unpublished data) were similar to those observed with wt GFP–X-PAK5 (Fig. 4). Thus, X-PAK5 kinase activity is not required to induce MT stabilization. No major reorganization of the actin network was detected with the kinase dead mutant (Fig. 9 B).

Most of the XTC cells expressing the active kinase displayed striking morphological changes with a retracted and often rounded cell body and very long cytoplasmic extensions (up to 50 μm long). In most of these cells, numerous filipodia were induced. The active kinase was either diffuse in the cytoplasm or expressed in many bright vesicles, some of which decorated few MTs. However, the active kinase was never seen distributing as filament along the entire length of the MTs (Fig. 9 C). The retraction of these cells complicated MTs analysis, since MTs could not spread well within the lamellae. Nevertheless, active kinase-expressing cells never contained the characteristic X-PAK5–bound curly MTs (Fig. 9 C). Virtually no stress fibers were detected in these cells (Fig. 9 C), which is consistent with previous reports showing that kinase active PAK1 and PAK4 induce stress fibers dissolution (Qu et al., 2001).

In summary, only catalytically inactive X-PAK5 possesses MT stabilization properties, and catalytic activation either results in the release of the kinase from the MTs or prevents its binding to the MTs. This raised the exciting possibility that upstream regulators of X-PAK5 kinase activity could control its MT stabilizing functions.

Cdc42 and Rac1 do not regulate X-PAK5 kinase activity but prevent its MTs binding

Because PAKs are regulated by small GTPases, we wished to assess whether Rac and/or Cdc42 may be responsible for X-PAK5 catalytic activation.

We first verified that X-PAK5 interacts with GTP-loaded Rac and Cdc42 and that binding occurs through the modified CRIB domain as described for hPAK4 (unpublished data). Next, constitutively active forms (V12) of Cdc42 or

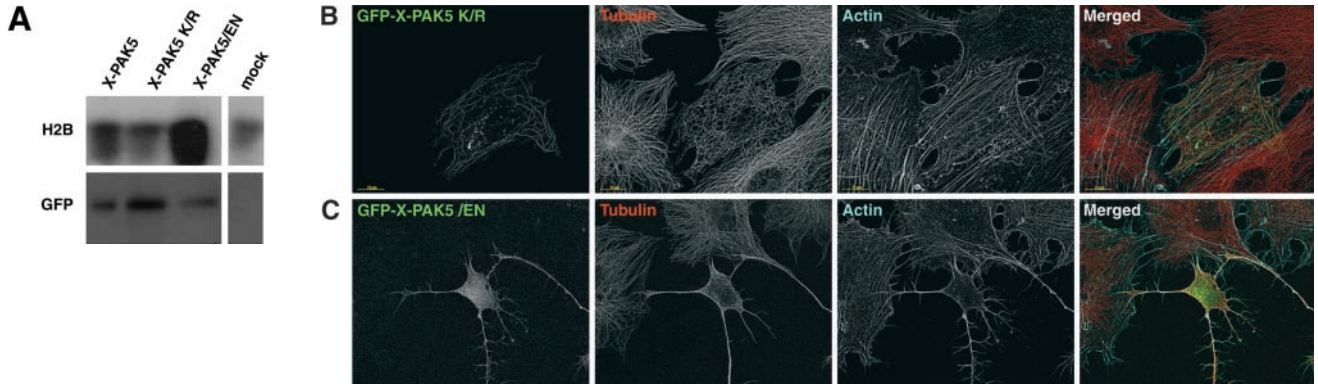

Figure 9. **Activities and subcellular localization of GFP–X-PAK5 mutants.** (A) In vitro kinase activity of mock or GFP–X-PAK5–, -K/R–, -EN–transfected cells. (Top) Kinase activity was tested against histone H2B substrate. (Bottom) Western blot of the immunoprecipitates using a GFP antibody. (B and C) XTC cells were transfected with GFP–X-PAK5 K/R (B) and GFP–X-PAK5/EN (C) and were costained for actin (blue) and tubulin (red).

Rac1 and GFP–X-PAK5 were cotransfected in XTC cells. Cdc42 and Rac1 did not regulate X-PAK5 catalytic activity, since no significant reproducible increase in H2B phosphorylation could be detected upon GFP–X-PAK5 coexpression with active GTPases (Fig. 10 A).

Next, we checked whether the active GTPases could regulate X-PAK5 subcellular localization. Coexpression of X-PAK5 with either Cdc42V12 or RacV12 resulted in its significant relocalization throughout the cell and to GTPases-dependent actin-rich regions (Fig. 10 B). More specifically, in cells coexpressing active Cdc42, X-PAK5 distributed to filipodia and small lamellipodia (Fig. 10 B), whereas in cells coexpressing active Rac1, X-PAK5 was nuclear and in the lamellipodia (Fig. 10 B). Although the MT network was still altered upon GTPases and X-PAK5 coexpression, MTs never had the curly morphology of X-PAK5–bound MTs (Fig. 10 B). Thus, although active Rac and Cdc42 do not significantly enhance X-PAK5 kinase activity they either prevent its binding to the MTs or displace it from the MTs to actin-rich structures (Fig. 10 C).

To further confirm this result, we used a biochemical approach. *Xenopus* egg extracts were incubated with either GST or GST-Cdc42V12 proteins, and the MT-associated protein fraction was further purified (as in Fig. 3). Most of endogenous X-PAK5 did not bind the MT/MAP fraction when the egg extract was preincubated with GST-Cdc42V12, whereas incubation with GST control did not affect X-PAK5 binding (Fig. 10 D), further confirming that Cdc42V12 prevents X-PAK5 binding to the MTs.

Discussion

In the present study, we cloned a novel kinase, X-PAK5, belonging to the hPAK4/hPAK6 subfamily of PAK that is known to function in protection against apoptosis, regulation of cell adhesion, and binding to the androgen receptor (Gnesutta et al., 2001; Qu et al., 2001; Yang et al., 2001).

X-PAK5 has a complex subcellular distribution. Indeed, it presents the unique feature to colocalize with both the actin and MT networks. Most importantly, the subset of X-PAK5 that binds the MTs network is regulated as cell cycle progresses. Like the endogenous kinase, ectopic GFP–X-PAK5 has a subcellular distribution that is targeted either to the actin or the MT networks. Once on the MT network, GFP–X-PAK5 induces a reorganization of the cell cytoskeleton. We investigated the relationship of this novel kinase with the dynamic of MTs.

Ectopic X-PAK5 reorganizes the MT network

We demonstrate that X-PAK5 is a MAP that directly binds the MTs. MTs bound by ectopically expressed X-PAK5 are thick and curly, mostly forming whorls around the nucleus. Under these conditions, few MTs appear to nucleate from the centrosome, which results in the apparent loss of the MT aster around the centrosome. Such a behavior was described previously for other MAPs (Kaech et al., 1996; Palazzo et al., 2001), and it would be of interest to test whether it may reflect a change in the centrosome activity. GFP–X-PAK5 is bound to a specific subset of both Tyr and GluMTs. The Tyr-MTs appear more peripheral, whereas Glu-MTs are often trapped around the nucleus. This distribution might explain the retraction of IF we observed in transfected cell, since IFs were shown to follow the path of GluMTs (Gurland and Gundersen, 1995).

Ectopic X-PAK5 binding to the MTs induces their stabilization and a paused state

We demonstrate that X-PAK5–bound MTs are stabilized by their interaction with the kinase. Indeed, X-PAK5–bound MTs are strongly resistant to NZ treatment. X-PAK5 binds dynamic MTs that are newly nucleating from the centrosome, and its binding to these MTs induced their paused state by preventing elongation/shortening and thus the development of a fully spread MT network. Finally, after cytoplasmic dilution some Tyr-positive X-PAK5–bound MTs remained labeled in X-PAK5–transfected cells when all Tyr-labeled MTs had vanished in the surrounding untransfected cells, again indicating that X-PAK5 binding contributes to MTs stabilization.

MAPs usually affect the dynamic parameters by either decreasing the catastrophe or increasing rescue frequencies and modulating the growth/shrinkage rates. Consequently, their depletion or overexpression results in either a dramatic shortening or lengthening of the MTs nucleating from the centrosome (for review see Andersen, 2000).

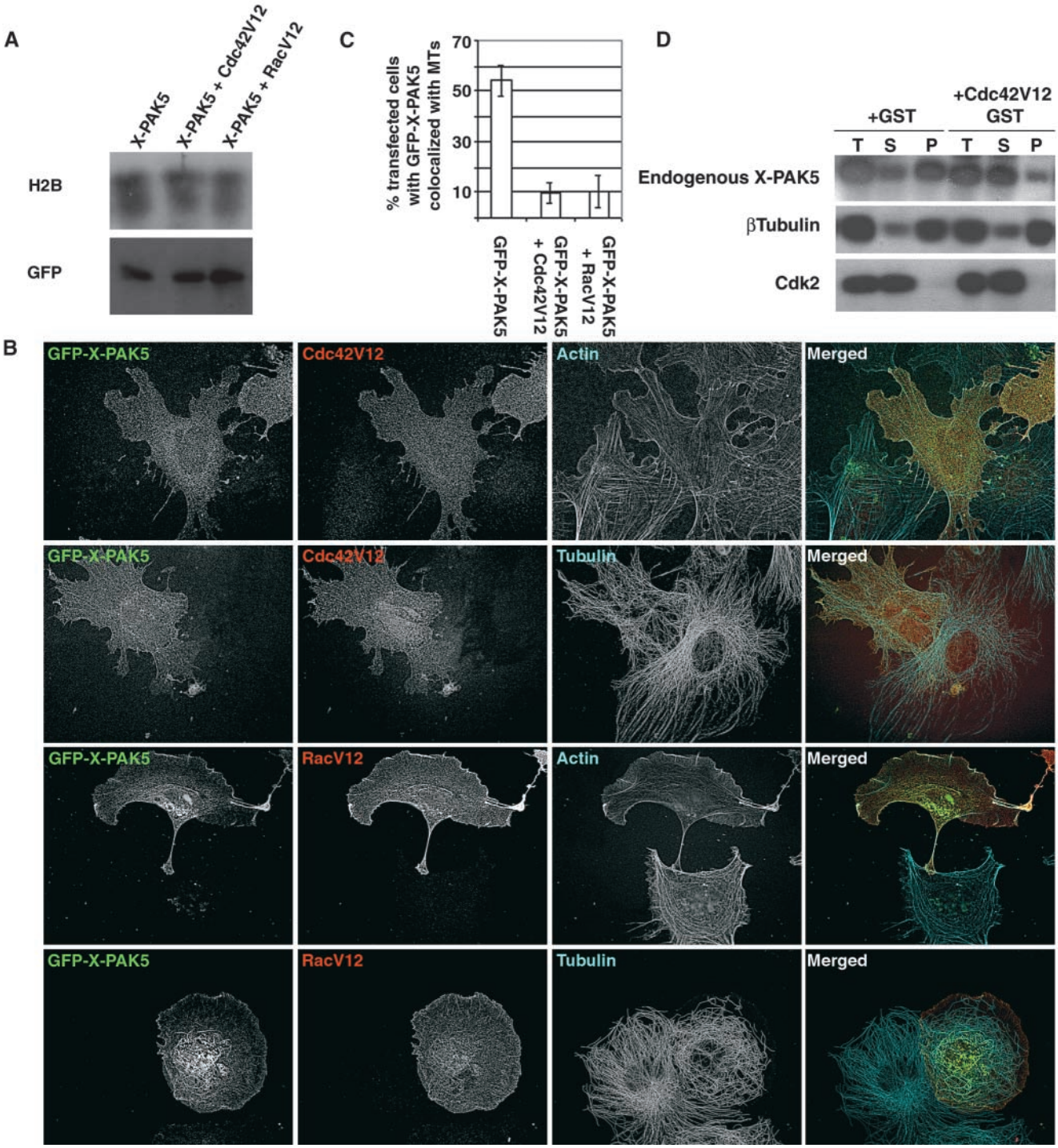

Figure 10. **X-PAK5 kinase is not activated but relocalizes upon GTPase expression.** XTC cells were cotransfected with GFP–X-PAK5 and pMT-mycCdc42V12 or -RacV12. (A, top) Kinase activities were assayed over H2B. (A, bottom) Western blot of the immunoprecipitates using a GFP antibodies indicates that equal amount of kinase were immunoprecipitated. (B) Representative myc-tagged active GTPase and GFP–X-PAK5–coexpressing cells were stained for GFP–X-PAK5 (green), GTPases using myc polyclonal antibody (Red), and tubulin antibodies or actin (blue, respectively). Merged micrographs are on the right. (C) Quantification of cells that present GFP–X-PAK5 binding to the MTs in cells expressing either GFP–X-PAK5 alone or coexpressed with active GTPases. In cells in which GFP–X-PAK5 still binds few MTs (like in B with RacV12), the GTPase is also bound to these few MTs. (D) Western blot analysis of MTs copelleting assays as in Fig. 3. Egg extracts were incubated for 30 min with purified GST or CDC42V12-GST prior to MT pelleting. Cdc42V12GST but not GST prevents most of X-PAK5 binding to the MT fraction (P).

In contrast, we show clearly that ectopic X-PAK5 strongly interferes with both the MTs elongation and shortening velocities and increases the time MTs spend in a paused state. This unusual behavior for a MAP results in a loss of the MT dynamic instability but does not severely affect the MTs length in the cell.

Interestingly, a similar activity was described recently when the RhoA pathway is turned on by LPA in serum-starved

NIH3T3 (Cook et al., 1998). In these cells, activation of mDia and ROKα also induces the selective stabilization of only a subset of MTs and results in their paused state (Palazzo et al., 2001). X-PAK5–bound MTs are curly and essentially surround the nucleus, and they resemble ROKα- rather than mDia-induced GluMTs. Moreover, activation of ROKα by RhoA and induction of perinuclear Glu-MTs also lead to vimentin collapse (Sin et al., 1998). Infante et al. (2000) demonstrated that this subset of MTs are stabilized by an ATP-sensitive cap that prevents incorporation of fresh tubulin subunits and the release of tubulin from the polymer, resulting in paused MTs that are subsequently detyrosinated. Taken together, these results suggest that the X-PAK5 and RhoA pathways may be intertwined, and it would be of interest to check whether X-PAK5 may participate to the MTs capping required for their stabilization. Furthermore X-PAK5, like RhoA effectors, belongs to a new MAP subfamily that only target a subpopulation of MTs. This clearly contrasts with "conventional" MAPs that stabilize the entire population of MTs.

Although we yet have to determine the biological significance of X-PAK5–induced curly MTs, we hypothesize that the induced paused state of a subset of MTs might be important for specific events such as cytokinesis, polarization, or cell migration.

What could be the physiology for paused and/or morphologically modified MTs?

X-PAK5–bound MTs are curly and display many bends. In neurons, two different types of MT behavior were reported that resemble what we observe with ectopic X-PAK5–bound MTs. First, when growth cones respond to extracellular cues and change their morphology to turn MTs bundle and bend (Tanaka and Kirschner, 1995). Second, a cage of stable MTs was observed surrounding the nucleus of migrating neurons (Rivas and Hatten, 1995) and was proposed to play a role in migration. Further investigations will be required to test whether X-PAK5, an abundant protein in the neural tissue, may play a function in these behaviors when it binds to MTs.

Low doses of NZ were shown to induce paused MTs by a loss of dynamic that might explain the low NZ dose-induced metaphase arrest (Vasquez et al., 1997). Interestingly, Bim1p, a yeast member of the EB1 family proteins, promotes the increased MTs dynamic required in G1 to position the spindle for mitosis entry (Tirnauer et al., 1999), and Bim1p deletion results in more time spent in the paused state. Although X-PAK5 binding to MTs increases in G2 phase, it is unclear whether it may represent a difference in G1/G2 MTs stability or whether X-PAK5 may participate to G2/M transition or in mitotic progression. Further work will be required to address these questions, since previous reports involved the PAK family in the regulation of cell cycle progression (Faure et al., 1997).

Functions of catalytically active and inactive X-PAK5

Here, we show that catalytically inactive X-PAK5 functions in binding and reorganizing MTs, whereas a kinase constitutive mutant loses its ability to bind MTs. Lin et al. (2000) also demonstrated recently that another kinase, DCAMKL1, is a MAP that induces MTs stabilization by a mechanism that is not dependent on its kinase activity.

Like for many other MAPs, X-PAK5 binding to the MTs is therefore negatively regulated by phosphorylation. We do not know whether X-PAK5 kinase phosphorylation and activation occurs on the MTs and results in its subsequent release. Such experiments have been hampered by the lack of known X-PAK5 kinase activators. However, it is interesting to note that once bound to focal adhesions catalytically active PAKs were shown to induce their dissolution, whereas kinase dead PAK increased focal adhesions (Kiosses et al., 1999). If X-PAK5 activation occurs on MTs, this may result in MT changes (e.g., suppress the kinase dead induced MT stabilization) and subsequently in the dramatic cell morphological changes and actin reorganization that are observed.

Catalytically active X-PAK5 induces the rounding/retraction of the cell body and the extension of long arborized processes that are often decorated with many filipodia. These changes always correlated with a complete dissolution of stress fibers. Thus, some of the actin rearrangements, dissolution of stress fibers, and filipodia induction mediated by catalytically active X-PAK5 are similar to those reported for the kinase active PAK4 (Qu et al., 2001). This was not unexpected, since both proteins essentially differ by the unique and highly charged 103 amino acids long region of X-PAK5. This domain is required for MT binding (unpublished data), which may explain why hPAK4 was not reported as a MAP. The dramatic changes of the cell morphology that are induced by catalytically active X-PAK5 were not described for hPAK4 and may again reflect the expression of the charged X-PAK5 insert or the different cell types used. Other mammalian PAK4 sequences likely arising from alternative splicing are described in the data banks and could likely be tissue specific. Indeed, we identified a 75-kD product in mouse brain and testis that specifically reacts with Abn122 (unpublished data).

X-PAK5 localization is regulated by the GTPases

In contrast to other PAKs, X-PAK5 not only mediates actin but also MTs rearrangements. Our results raised the exciting possibility that X-PAK5 could act downstream of RhoA as an inactive kinase and downstream of small GTPases binding to the CRIB motif as an active kinase. However, we were unable to demonstrate any clear relationship between RhoA pathways and X-PAK5 (unpublished data). Nevertheless, although active Cdc42, and to a lesser extent Rac, bound X-PAK5 they did not induce kinase activation as was also described for hPAK4 (Abo et al., 1998). Upon their coexpression, X-PAK5 relocated mainly to the Cdc42- and Rac-induced actin-rich regions, and cell morphology was typical of active GTPase-expressing cells, rather than the morphology of catalytically active X-PAK5–expressing cells. Indeed, new GTPases keep being identified, and although X-PAK5 interacts with active Cdc42 and Rac they may not be the X-PAK5 preferred/chosen partner in physiological conditions.

In summary, we identified a new member of the PAK family that displays the remarkable properties of binding to both the MT and the actin networks. Catalytically inactive X-PAK5 has a strong affinity for MTs, and we hypothesize that after interaction with different partners (e.g., GTPases) or catalytic activation a change of conformation will release X-PAK5 from MTs and will provide a new affinity for the actin cytoskeleton.

In this regard, the identification of upstream regulators of X-PAK5 that directs it to stress fibers, filipodia, lamellipodia, or MTs will provide a better understanding in the coordination of the MT and actin cytoskeletons that is crucial for cell morphology and motility.

Materials and methods

X-PAK5 cDNA cloning and expression vectors

A partial X-PAK5 cDNA was obtained (Faure et al., 1997) and its 5′ end cloned according to the Marathon 5′ RACE protocol (CLONTECH Laboratories, Inc.). The full-length clone subcloned in pEGFP, pDs-Red, and pRSET vectors (CLONTECH Laboratories, Inc.). X-PAK5 subdomains, X-PAK5Nter (amino acids 2–378), X-PAK5n122 (amino acids 122–224), and kinase domain (amino acids 379–649) were subcloned in pEGFP and pGEX4T. All pEGFP–X-PAK5 constructs were subcloned as GFP fusions in pCS2 plasmids (D. Turner and R. Rupp, Fred Hutchinson Cancer Center, Seattle, WA) to allow transcription/translation in reticulocyte lysates (Promega). X-PAK5–K/R dead and X-PAK5/EN constitutive kinase mutants were constructed by site-directed mutagenesis (Faure et al., 1997). The following changes were made: K to R at residue 409 located in the putative ATP binding site for the kinase dead mutant and S to E and S to N at residues 504 and 533 for the EN constitutive mutant, respectively. All constructs were verified by sequencing.

Antibodies, Western blots, and kinase activities

Monoclonal antibodies to β-tubulin (used to label all MTs, E7) and to IFs (14H7) are from the DSHB (Iowa State University, Iowa City, IA). 14H7 were used in Fig. 2 (with Abn122 for X-PAK5 and rat Yol3/4 [Serotec] for α-tubulin). YL1/2 (Kilmartin et al., 1982) and L3 antibodies (Paturle-Lafanechere et al., 1994) are against TyrMTs and GluMTs. Polyclonal antibody to vimentin (no. 314), a gift from Dr. Robert D. Goldman (Northwestern University Medical School, Chicago, IL), were used to stain IFs (with E7) in Fig. 4. Cdk2 antibodies were a gift from Dr. Bonne-Andrea (Centre de Recherche de Biochimie Macromoleculaire). Antibodies against the amino acid 122–224 domain fused to GST of X-PAK5 (Abn122) were made and immunopurified in the lab (Faure et al., 1997). The specificity of X-PAK5 antibodies was confirmed by Western blot and immunofluorescence analysis and by signal quenching.

X-PAK5 Western blots and immunoprecipitates were performed with immunopurified antibodies. 100 μg of total tissue, egg, or *Xenopus* cell extracts was loaded on SDS-PAGE. For kinase activity, endogenous and mutant X-PAK5 were immunoprecipitated from 5×10^6 cells using Abn122 and activity measured as in Cau et al. (2000).

Cell culture, transfection, and light microscopy

Epithelial wt A6 or stably expressing GFP–β-tubulin (H1H10) tadpoles XTC and XL-2 *Xenopus* cell lines were used. Cells were transfected using Lipofectamine Plus reagent (GIBCO-BRL) for 24 h. DSP-Tsb fixative procedure was used to preserve cytoskeleton structures (Bell and Safiejko-Mroczka, 1995). However, in the experiment in Fig. 7 cold methanol was used. Coverslips were first incubated with primary antibodies in PTF buffer (PBS, 0.05% Triton X-100, and 5% FCS) and then with secondary antibodies conjugated either to Texas red, FITC, or biotin (Amersham Pharmacia Biotech); neutravidin-Alexa350 (Molecular Probes) was used. Actin and Golgi were visualized using CPITC or A350-conjugated phalloidin and FITC-Helix pomatia lectin. All incubations performed for 1 h were followed by extensive washes in PTF buffer.

Fixed cells were observed with either a confocal microscope (MRC 1024; Bio-Rad Laboratories) or a DMR A microscope PL APO 63× oil objective (1.32 NA) and the A4, GFP, N2.1 filter sets (Leica). Images were captured using a piezzo stepper (E662 LVPTZ amplifier; Servo) and a cooled CCD Micromax camera (1,300 × 1,030 pixels, RS; Princeton Instruments Inc.) driven by MetaMorph (v 4.5; Universal Imaging Corp.). Pixel sizes were 106 × 106 nm, and voxel sizes were 106 × 106 × 100 nm. For deconvolution and image reconstruction, xyz image stacks of fixed cells or xyt image stacks for live cells were processed on a SGI Octane workstation running Huygens 1 and 2.3 (Scientific Volume Imaging b.v.; Hilversum) using MLE and MLE time algorithms. Three-dimensional restored stacks were processed with Imaris 3.0 and Voxelshop Pro (Bitplane) for volume rendering and quantification.

Live cells (at 26.5°C) were observed with a DM IRBE inverted microscope with PL APO 63× oil objective (1.32 NA) using the setup described above (with a 2 × 2 binning, thus the resolution is 650 × 515 pixels). Images were taken at 1 image/3 s for single or 2 images/15 s for double transfected cells.

Quantification

For colocalization, image stacks were cropped and automatically thresholded using the select polygonal function. Colocalization analysis calculated for every plane of the stack was performed on Voxelshop Pro. Codistribution between protein A and B was considered significant when the percentage of A voxels colocalized with B was significantly larger than the relative area of the cell covered by B (in percent voxels).

Tyr/Glu ratio was measured using the Tyr and Glu antibodies. The Tyr and Glu fluorescence intensities of a single transfected cell were measured using the region measurements function of Metamorph 4.5. R1, the calculated Tyr/Glu ratio, was compared with R2, the average Tyr/Glu of untransfected cells of the same field. The R1/R2 value was plotted versus the GFP intensity of the transfected cell.

For time-lapse microscopy, free ends of filaments (MTs and bundles of MTs) were tracked using the track point function of Metamorph during an average of 5 min. The flatness of the *Xenopus* cell lines used allowed us to track the end of filaments without ambiguity. Values were transferred on Microsoft Excel 98, analyzed without filters using a macro, and dynamic parameters were calculated. Rescue and catastrophe frequencies were calculated by dividing the number of events of rescue/catastrophe of a single MT by the time of observation.

Cell synchronization

Because XTC cells synthesize growth factors that prevent cell cycle exit by starvation, XL2 cells were used for cell synchronization (Uzbekov et al., 1998).

Resistance of MTs to dilution

Transfected XTC cells were treated as in Cook et al. (1998), but PEM buffer contained only 0.2 mM EGTA, and EBSS buffer was replaced by PBS buffer. Cells were grown on fibronectin-coated coverslips.

MTs and actin binding assays

MTs were polymerized from high speed egg cytosolic extracts (HSS) (Morin et al., 1994). 100 μL HSS were incubated at 23°C for 30 min with either 25 μM taxol alone or with 10 μL in vitro–translated proteins. Reactions were layered on a 40% glycerol cushion in BRB80 (80 mM Pipes, pH 6.8, 1 mM EGTA, 1 mM $MgCl_2$, 1 mM GTP) containing 10 μM taxol and centrifuged (400,000 *g*) for 30 min at 25°C. Supernatants were saved, and pellets washed three times with BRB80 were resuspended in BRB80 containing 5 mM $CaCl_2$ and 300 mM NaCl. 2 μl equivalent of each fraction were separated by SDS PAGE, transferred to nitrocellulose, and sequentially probed with E7, Abn122, and anti-Cdk2Cter antibodies.

Tubulin was purified from porcine brain according to Hyman et al. (1991). Purified tubulin was polymerized at 30°C for 30 min in MEM buffer (50 mM MES, pH 6.7, 2 mM EGTA, 1 mM $MgCl_2$, 1 mM GTP, 25 μM taxol) containing 25% glycerol. Increasing quantities of purified His_6-tagged X-PAK5 were mixed to 20 μg in vitro–polymerized MTs and incubated at 37°C for 30 min. The MTs/His_6-tagged X-PAK5 mix was laid over a cushion of MEM containing 10% sucrose and centrifuged at 50,000 *g* at 37°C for 30 min. Pellets were washed three times with warm MEM. Pellets and supernatants separated by SDS-PAGE were stained with Coomassie blue.

F-actin was incubated (0.1 nmol) for 30 min with 10 μl of in vitro–translated GFP–X-PAK5 mutants in Ac buffer (20 mM Tris, 100 mM KCl, 2 mM $MgCl_2$, pH 7.4) before ultracentrifugation for 20 min at 100,000 *g* at 4°C. Pellets were washed three times in Ac buffer. Total (T), depleted supernatant (S), and pellets (P) separated by PAGE-SDS and autoradiographed (for X-PAK5) and Coomassie stained (for actin).

Online supplemental material

Videos 1 and 2 accompany Fig. 7 B. Videos 3, 4, and 5 accompany Fig. 8. Videos available at http://www.jcb.org/cgi/content/full/jcb.200104123/DC1.

The authors wish to thank Dr. Travo, head of the Integrated Imaging Facility of the Laboratory, for his constant interest and support. We especially thank Drs. Tsukita and Mimori-Kiyosue (Tsukita Cell Axis Project, ERAT, Japan Science and Technology Corp., and Kyoto University, Kyoto, Japan) for their gift of the H1H10 cell line. We acknowledge N. Lautredou for assistance with confocal images and S. Vigneron and C. Donier for technical assistance. We are grateful to Drs. Chaussepied, Lafanéchère, Eddé, Gauthier–Rouviere, Prigent, Bonne-Andréa, Goldman, and Job for fruitful discussions and gift of reagents. We want to acknowledge Dr. B. Hipskind

for critical reading of the article.

This work was supported by a grant from the Association pour la Recherche sur le Cancer (to N. Morin)

Submitted: 26 April 2001
Revised: 17 October 2001
Accepted: 19 October 2001

References

Abo, A., J. Qu, M.H. Cammarano, C. Dan, A. Fritsch, V. Baud, B. Belisle, and A. Minden. 1998. PAK4, a novel effector for Cdc42Hs, is implicated in the reorganization of the actin cytoskeleton and in the formation of filopodia. *EMBO J*. 17:6527–6540.

Andersen, S. 2000. Spindle assembly and the art of regulating microtubule dynamics by MAPs and Stathmin/op18. *Trends Cell. Biol.* 10:261–267.

Bagrodia, S., and R.A. Cerione. 1999. Pak to the future. *Trends Cell Biol.* 9:350–355.

Bell, P.B., and B. Safiejko-Mroczka. 1995. Improved methods for preserving macromolecular structures and visualizing them by fluorescence and scanning electron microscopy. *Scanning Microscopy*. 9:843–860.

Best, A., S. Ahmed, R. Kozma, and L. Lim. 1996. The Ras-related GTPase Rac1 binds tubulin. *J. Biol. Chem.* 271:3756–3762.

Cau, J., S. Faure, S. Vigneron, J.C. Labbé, C. Delsert, and N. Morin. 2000. Regulation of X-PAK2 by Cdc42 and MPF controls *Xenopus* oocyte maturation. *J. Biol. Chem*. 275:2367–2375.

Cook, T.A., T. Nagasaki, and G.G. Gundersen. 1998. Rho guanosine trisphosphatase mediates the selective stabilization of MTs induced by lysophosphatidic acid. *J. Cell Biol.* 141:175–185.

Daniels, R.H., and G.M. Bokoch. 1999. p21-activated protein kinase: a crucial component of morphological signaling? *Trends Biochem. Sci.* 24:350–355.

Daub, H., K. Gevaert, J. Vandekerckhove, A. Sobel, and A. Hall. 2001. Rac/Cdc42 and p65PAK regulate the microtubule-destabilizing protein stathmin through phosphorylation at serine 16. *J. Biol. Chem.* 276:1677–1680.

Edwards, D.C., L.C. Sanders, G.M. Bokoch, and G.N. Gill. 1999. Activation of LIM-kinase by Pak1 couples Rac/Cdc42 GTPase signalling to actin cytoskeletal dynamics. *Nat. Cell. Biol*. 1:253–259.

Enomoto, T. 1996. MT disruption induces the formation of actin stress fibers and focal adhesions in cultured cells: possible involvement of the rho signal cascade. *Cell Struct. Funct.* 21:317–326.

Etienne-Manneville, S., and A. Hall. 2001. Integrin-mediated activation of Cdc42 controls cell polarity in migrating astrocytes through PKCzeta. *Cell.* 106: 489–498.

Faure, S., S. Vigneron, M. Doree, and N. Morin. 1997. A member of the Ste20/PAK family of protein kinases is involved in both arrest of *Xenopus* oocytes at the G2/prophase of the first meiotic cell cycle and in prevention of apoptosis. *EMBO J.* 18:5550–5561.

Faure, S., S. Vigneron, S. Galas, T. Brassac, C. Delsert, and N. Morin. 1999. Control of G2/M transition in *Xenopus* by a member of the PAK family: a link between PKA and PAK signalling pathways? *J. Biol. Chem.* 274:3573–3579.

Gnesutta, N., J. Qu, and A.G. Minden. 2001. The serine/threonine kinase PAK4 prevents caspase activation and protects cells from apoptosis. *J. Biol. Chem.* 276:14414–14419.

Gurland, G., and G.G. Gundersen. 1995. Stable, detyrosinated microtubules function to localize vimentin intermediate filaments in fibroblasts. *J. Cell Biol.* 131:1275–1290.

Hyman, A., D. Drechsel, D. Kellogg, S. Salser, K. Sawin, P. Steffen, L. Wordeman, and T. Mitchison. 1991. Preparation of modified tubulins. *Methods Enzymol*. 196:478–485.

Infante, A.S., M.S. Stein, Y. Zhai, G.G. Borisy, and G.G. Gundersen. 2000. Detyrosinated (Glu) microtubules are stabilized by an ATP-sensitive plus-end cap. *J. Cell Sci.* 113:3907–3919.

Kaech, S., B. Ludin, and A. Matus. 1996. Cytoskeletal plasticity in cells expressing neuronal microtubule-associated proteins. *Neuron.* 17:1189–1199.

Kaverina, I., K. Rottner, and J.V. Small. 1998. Targeting, capture, and stabilization of MTs at early focal adhesions. *J. Cell Biol.* 142:181–190.

Kaverina, I., O. Krylyshkina, and J.V. Small. 1999. MT targeting of substrate contacts promotes their relaxation and dissociation. *J. Cell Biol.* 146:1033–1044.

Kilmartin, J.V., B. Wright, and C. Milstein. 1982. Rat monoclonal antitubulin antibodies derived by using a new nonsecreting rat cell line. *J. Cell Biol.* 93: 576–582.

Kiosses, W.B., R.H. Daniels, C. Otey, G.M. Bokoch, and M.A. Schwartz. 1999. A role for p21-activated kinase in endothelial cell migration. *J. Cell Biol.* 147: 831–844.

Lin, P.T., J.G. Gleeson, J.C. Corbo, L. Flanagan, and C.A. Walsh. 2000. DCAMKL1 encodes a protein kinase with homology to doublecortin that regulates microtubule polymerization. *J. Neurosci.* 20:9152–9161.

Manser, E., and L. Lim. 1999. Roles of PAK family kinases. *Prog. Mol. Subcell. Biol.* 22:115–133.

Manser, E., T. Leung, H. Salihuddin, Z.S. Zhao, and L. Lim. 1994. A brain serine/threonine protein kinase activated by Cdc42 and Rac1. *Nature.* 367:40–46.

Mimori-Kiyosue, Y., N. Shiina, and S. Tsukita. 2000. The dynamic behavior of the APC-binding protein EB1 on the distal ends of microtubules. *Curr. Biol.* 10:865–868.

Morin, N., A. Abrieu, T. Lorca, F. Martin, and M. Dorée. 1994. The proteolysis-dependent metaphase to anaphase transition: calcium/calmodulin-dependent protein kinase II mediates onset of anaphase in extracts prepared from unfertilized *Xenopus* eggs. *EMBO J.* 13:4343–4352.

Nagasaki, T., C.J. Chapin, and G.G. Gundersen. 1992. Distribution of detyrosinated microtubules in motile NRK fibroblasts is rapidly altered upon cell-cell contact: implications for contact inhibition of locomotion. *Cell Motil. Cytoskeleton*. 23:45–60.

Nobes, C.D., and A. Hall. 1995. Rho, Rac, and Cdc42 GTPases regulate the assembly of multimolecular focal complexes associated with actin stress fibers, lamellipodia, and filopodia. *Cell.* 81:53–62.

Ohtakara, K., H. Inada, H. Goto, W. Taki, E. Manser, L. Lim, I. Izawa, and M. Inagaki. 2000. p21-activated kinase PAK phosphorylates desmin at sites different from those for Rho-associated kinase. *Biochem. Biophys. Res. Commun.* 272:712–716.

Palazzo, A.F., T. Cook, A.S. Alberts, and G.G. Gundersen. 2001. mDia mediates Rho-regulated formation and orientation of stable microtubules. *Nat. Cell Biol.* 3:723–729.

Paturle-Lafanechere, L., M. Manier, N. Trigault, F. Pirollet, H. Mazarguil, and D. Job. 1994. Accumulation of delta 2-tubulin, a major tubulin variant that cannot be tyrosinated, in neuronal tissues and in stable MT assemblies. *J. Cell Sci.* 107:1529–1543.

Qu, J., M. Cammarano, Q. Shi, K.C. Ha, P. de Lanerolle, and A. Minden. 2001. Activated PAK4 regulates cell adhesion and anchorage-independent growth. *Mol. Cell. Biol.* 10:3523–3533.

Rivas, R.J., and M.E. Hatten. 1995. Motility and cytoskeletal organization of migrating cerebellar granule neurons. *J. Neurosci.* 15:981–989.

Sin, W.C., X. Chen, T. Leung, and L. Lim. 1998. RhoA-binding kinase alpha translocation is facilitated by the collapse of the vimentin intermediate filament network. *Mol. Cell. Biol.* 18:6325–6339.

Tanaka, E., and M.W. Kirschner. 1995. The role of microtubules in growth cone turning at substrate boundaries. *J. Cell Biol.* 128:127–137.

Tirnauer, J., E. O'Toole, L. Berrueta, B. Bierer, and D. Pellman. 1999. Yeast Bim1p promotes the G1-specific dynamics of microtubules. *J. Cell Biol.* 145:993–1007.

Uzbekov, R., I. Chartrain, M. Philippe, and Y. Arlot-Bonnemains. 1998. Cell cycle analysis and synchronization of the *Xenopus* cell line XL2. *Exp. Cell. Res.* 242:60–68.

Vadlamundi, R.K., L. Adam, R.A. Wang, M. Mandal, D. Nguyen, A. Sahin, J. Chernoff, M. Hung, and R. Kumar. 2000. Regulatable expression of p21-activated kinase-1 promotes anchorage-independent growth and abnormal organization of mitotic spindles in human epithelial breast cancer cells. *J. Biol. Chem.* 275:36238–36244.

Vasquez, R.J., B. Howell, A.M. Yvon, P. Wadsworth, and L. Cassimeris. 1997. Nanomolar concentrations of nocodazole alter microtubule dynamic instability in vivo and in vitro. *Mol. Biol. Cell.* 8:973–985.

Waterman-Storer, C.M., R.A. Worthylake, B. Liu, K. Burridge, and E.D. Salmon. 1999. MT growth activates Rac1 to promote lamellipodial protrusion in fibroblasts. *Nat. Cell Biol.* 1:45–50.

Yang, F., X. Li, M. Sharma, M. Zarnegar, B. Lim, and Z. Sun. 2001. Androgen receptor specifically interacts with a novel p21-activated kinase, PAK6. *J. Biol. Chem*. 276:15345–15353.

Zeng, Q., D. Lagunoff, R. Masaracchia, Z. Goeckeler, G. Cote, and R. Wysolmerski. 2000. Endothelial cell retraction is induced by PAK2 monophosphorylation of myosin II. *J. Cell Sci.* 11:471–482.